Journal of Hazardous Materials 447 (2023) 130794

Contents lists available at ScienceDirect

Journal of Hazardous Materials

journal homepage: www.elsevier.com/locate/jhazmat

The chlorination of glycine and α-alanine at excess HOCl: Kinetics and mechanism

Fruzsina Simon [a,b], Mária Szabó [a,b,*], István Fábián [a,b]

[a] Department of Inorganic and Analytical Chemistry, University of Debrecen, Debrecen, Hungary
[b] ELKH - DE Mechanisms of Complex Homogeneous and Heterogeneous Chemical Reactions Research Group, University of Debrecen, Debrecen, Hungary

HIGHLIGHTS

- The chlorination mechanisms of glycine and alanine at HOCl excess is explored.
- Antagonistic products and intermediates were identified in these systems.
- At high pH, the formation of *N*,*N*-dichloroamino acid does not occur.
- At pH ~ 7, Cl_2O chlorinates monochloroamino acid to produce dichloroamino acid.
- The CH_3 group on the α-carbon atom profoundly alters the chlorination mechanism.

GRAPHICAL ABSTRACT

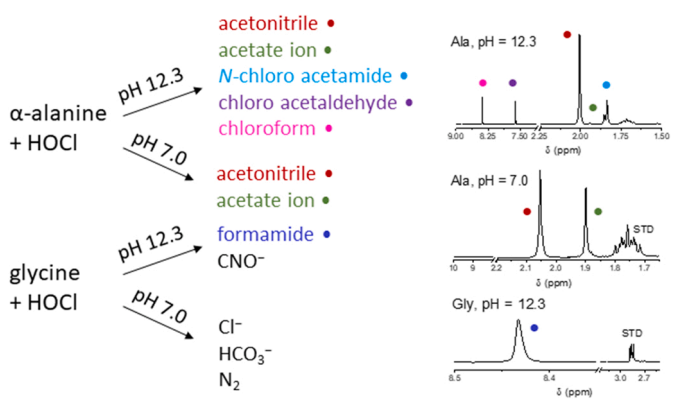

ARTICLE INFO

Editor: Dr. C. Baiyang

Keywords:
Kinetics
N-chloroglycine
N-chloroalanine
Oxidation
Hypochlorous acid
Chlorination

ABSTRACT

The chlorination of the two simplest amino acids at HOCl excess was studied by stopped-flow, conventional spectrophotometric and time resolved ^{1}H NMR kinetic methods at 25 °C. These reactions show distinct characteristics under neutral and alkaline conditions. At high pH, the common feature of the two systems is that the *N*-dichloroamino carboxylate ion does not form and the overall process is controlled by the initial decomposition of the *N*-monochloro derivative. Under such conditions, carbanions form in equilibrium acid – base processes and open alternative reaction paths, resulting in enhanced complexity of the corresponding mechanisms. In the case of α-alanine, the formation of acetonitrile and *N*-chloro acetamide as main products; acetate ion, acetaldehyde, chloroacetaldehyde, chloroform as byproducts; acetamide and *N*-chloro ethanimine as intermediates was confirmed. In the case of glycine, the final products are formamide and OCN^-. Under neutral conditions, monochloroamino acid forms immediately upon mixing the reactants, and subsequently it is converted into dichloroamino acid by Cl_2O in a fast process. In considerably slower further reaction steps, acetonitrile and acetate ion form as final products in the α-alanine system, while the chlorination of glycine proceeds to full mineralization. The detailed mechanisms suggested for these reactions postulate the formation of various imines and *N*-chloro imines which are involved in decarboxylation, dechlorination, hydration and hydrolytic reaction steps.

* Corresponding author at: Department of Inorganic and Analytical Chemistry, University of Debrecen, Debrecen, Hungary.
E-mail address: szabo.maria@science.unideb.hu (M. Szabó).

https://doi.org/10.1016/j.jhazmat.2023.130794
Received 22 October 2022; Received in revised form 8 January 2023; Accepted 12 January 2023
Available online 13 January 2023
0304-3894/© 2023 The Authors. Published by Elsevier B.V. This is an open access article under the CC BY-NC-ND license (http://creativecommons.org/licenses/by-nc-nd/4.0/).

1. Introduction

Powerful oxidants such as ozone, chlorine, hypochlorous acid, chlorine dioxide, and chloramines are well-known disinfectants and commonly utilized in water treatment processes [47]. Owing to its low cost, chlorine is the most frequently used oxidizing agent in drinking water technologies. Chlorine exists as the equilibrium mixture of the following forms in aqueous medium: Cl_2, Cl_2O, HOCl, OCl^-, and the concentration ratios of these species are controlled by the pH and the chloride ion concentration. In this paper, always HOCl is mentioned and the different forms are distinguished only when it is required for sake of clarity. Hypochlorous acid is involved in a variety of side reactions with the dissolved organic contaminants of source waters which may produce antagonistic disinfection by-products (DBPs).[1,23,24,26,38,39,5,50] The formation of halogenated organic compounds, most notably trihalomethanes (THMs) [12,17,20,27,28,36] and adsorbable organic halides (AOXs) [37,49], are of primary concern in drinking water technologies. The stability and biological activity of these compounds are not explored in sufficient detail. In some cases, these products are quite resistant against further transformations and may persist in the treated water for hours or days [9].

In earlier studies, organic chloramines have been shown to cause significant protein and DNA damage, inhibit DNA self-healing, affect cell life cycle, and ultimately induce apoptosis under biological conditions [12,17,27,36]. These are the common characteristics of carcinogens. The exact mechanism of their toxicity is not well known but they showed greater cytotoxicity and genotoxicity than chlorinated trihalomethanes and haloacetic acids. [20].

The concentration of amino acids in natural waters is between 20 and 10000 μg/L, and may account for up to 13% of dissolved carbon and 75% of dissolved organic nitrogen [44,46]. According to our recent results, the chlorination reactions of glycine and α-alanine are expected to show distinct features due to the α-methyl group in α-alanine [40]. Szabo et al. [42]. In addition, glycine and α-alanine are among the most abundant amino acids in various source waters [10,18,48]. Thus, detailed mechanistic studies on their chlorination is highly relevant. Chloramines formed from amino acids are relatively unstable. It requires relatively long time that the finished water reaches the consumer after chlorination, thus they are most likely exposed to the decomposition products of organic chloramines rather than to the parent compounds. To fully understand the health effects of the formation of *N*-chloroamino acids in drinking water technologies, the products and by-products of the reactions of amino acids with hypochlorous acid need to be identified and the corresponding reaction mechanisms need to be explored in detail [21]. Beside the fact that the by-products of disinfection are potentially harmful to human health, their presence is also associated with taste and odor issues. Cai et al, [22,47,6,7] In this respect, it is important to note that the costumers often judge the quality and the safety of drinking water by considering such properties [22].

The excess of hypochlorous acid generates dichloroamino acids during the chlorination of raw water. Their decomposition may lead to the formation of aldehydes and *N*-chloraldimines. The latter compounds are often considered as intermediates in nitrile formation [6,7]. Although non-halogenated nitriles do not have unpleasant odor, they have been found to be more toxic than the corresponding aldehydes because hydrogen cyanide is released during their metabolism [16,30,8]. Volatile carboxylic acids resulting from the oxidation of aldehydes can also have unpleasant odor with an odor threshold of 0.007–0.27 mM [19].

Glycine is an important precursor of cyanogen chloride (CNCl). Earlier, cursory kinetic experiments showed that CNCl formation was proportional to the rate of degradation of *N*, *N*-dichloro glycine. It was also suggested that the glycine nitrogen is stoichiometrically converted to CNCl above pH 6, while the conversion decreases at lower pH. Although the reaction has not been explored in detail, the results indicate that the formation of CNCl may be relevant in drinking water treatment [11,32–34].

To accurately assess the risks associated with the presence of organic chloramines in drinking water, it is important to explore both the formation mechanisms and stability of these compounds. Now we report a detailed study on the chlorination of glycine and α-alanine at HOCl excess in the neutral and the alkaline pH region. Our primary goal is to establish the detailed reaction sequence leading to the elimination of these amino acids from water. We wish to identify the final products and the intermediates formed over the course of the overall processes. Determining the lifetimes of these species in water may have outmost significance in predicting the adversary effects of the chlorination process. The results reveal important details of these reactions and provide useful chemical background for practical applications in water treatment and other chlorination technologies. The comparison of the results at two different pH regions offers a possibility to evaluate how acid-base reactions of the reactants affect the kinetics and the mechanistic features of these chlorination reactions.

2. Experimental

2.1. Chemicals and solutions

Analytical grade α-alanine, glycine, acetaldehyde, formaldehyde, formamide, acetonitrile, acetamide, acetaldehyde, chloroacetaldehyde, potassium-cyanate, potassium iodide (Sigma-Aldrich), acetic acid, chloroform (VWR), sodium carbonate (Reanal) were used without further purification. Chloride ion free sodium hypochlorite solutions were prepared, stored, and standardized as described earlier [2,35,40,42]. The pH was adjusted with NaOH solution in the alkaline region. The variation of the pH during the chlorination reaction was always negligible under this condition. Disodium hydrogen phosphate dihydrate (Sigma-Aldrich) and sodium dihydrogen phosphate dihydrate (Reanal) were used as buffers in the pH = 6 – 8 region. With the exceptions of the NMR and ion chromatographic measurements, all experiments were performed at constant ionic strength (1.0 M $NaClO_4$). $NaClO_4$ was prepared from perchloric acid and anhydrous Na_2CO_3 (Reanal) as described earlier [13]. The samples were prepared in doubly deionized and ultrafiltered water from a Purelab Classic (ELGA) water purification system.

2.2. Methods

Spectrophotometric studies were performed with Hewlett-Packard 8543 and Agilent Technologies Cary 8454 diode array spectrophotometers. The possibility of photochemical interference caused by the spectrophotometer was excluded by using different illumination protocols in repeated kinetic runs [14]. The temperature of the cell was controlled by a built-in thermoelectric Peltier device. Quartz cuvettes with different optical path lengths were used in the measurements, depending on the concentration of the reactants.

Rapid reactions were monitored with an Applied Photophysics SX20-MV stopped-flow instrument using a photomultiplier tube (PMT) as the detector. The kinetic traces were collected as the average of at least 3 runs using 10.0 mm optical path length. The dead time of the stopped-flow instrument – t_d = 1.51 ms – was determined by monitoring the reduction of 2,6-dichlorophenol-indophenol (DCPIP) under pseudo-first order conditions with ascorbic acid in excess [45].

pH measurement and potentiometric titrations were performed with a Metrohm 888 Titrando automatic titrator using Metrohm 6.0262.100 combined glass and Metrohm 6.0451.100 combined platinum electrodes. The readout of the pH meter was converted as described earlier, and pH = $-\log[H^+]$ thorough this paper [25]. The experimental data were evaluated using OriginPro 9.1 [31].

Ion chromatographic analysis was carried out by using a Thermo Scientific Dionex ICS-5000 + ion chromatograph equipped with an AS – DV Dionex autosampler, a gradient pump (Dionex ICS - 5000 DP), an

analytical CD Conductivity detector (Dionex ICS - 3000/5000) and a 4 mm anion self-regeneration suppressor (Dionex AERS) operated in the auto-suppression recycle mode. A Dionex IonPac AS19 4 × 250 mm analytical column was used in conjunction with a Dionex IonPac AG19 4 × 250 mm guard column. Isocratic elution was applied by using NaOH solution (0.020 M), the flow rate and the and column temperature were set at 1.0 mL × min^{-1} and 30 °C, respectively.

NMR measurements were performed on a Bruker DRX-400 MHz spectrometer. The unit is equipped with a VT-1000 temperature controller and a 5 mm z grad BBI head. The spectra were recorded using 32 scans with an acquisition time of 1.366 s and a 90° pulse. The results obtained from the experiments were evaluated using MestReNova and WinNMR programs. The spectra were recorded in aqueous solutions and the characteristic peak of water protons (4.8 ppm) was suppressed using a watergate pulse sequence (12.6 dB). [3,29] However, this is not entirely selective, so the peak intensities close to the watermark are smaller than expected but proportional to the concentration of the corresponding species. During the measurements, a capillary containing 0.0231 M aqueous solution of DSS (4,4-dimethyl-4-silapentane-1--sulfonic acid) was placed in the NMR tube as an external standard. This arrangement was necessary to avoid any interference by the standard in the chlorination reactions. In addition, it made possible the quantitative comparison of the concentrations of various compounds in different reaction mixtures. Shimming the instrument was made with the actual samples and took several minutes. Thus, the first spectrum could be recorded about 3 min after mixing the reactants in the time resolved NMR experiments.

3. Results and discussion

Preliminary experiments confirmed that the reactions show complex pH dependence and relatively simple kinetic behavior was observed only under neutral and highly alkaline conditions. Therefore, detailed studies were made at pH 7.0 and 12.3, but the combination of the corresponding results are also expected to provide information on the mechanisms in the intermediate pH range.

3.1. Alkaline conditions

The oxidation of glycine (Gly) and α-alanine (Ala) by excess HOCl exhibits composite kinetic features. Under alkaline conditions, a fast initial increase in the absorbance is followed by a relatively slow decay. The contribution of OCl^- to the absorbance is relatively small at the maxima of the characteristic absorption bands of mono-*N*-chloroglycine (MCG) and mono-*N*-chloro-α-alanine (MCA), 240 and 253 nm, respectively. Thus, the fast initial step could easily be monitored at these wavelengths. Simple first order kinetic traces were observed (Fig. S1) which were fitted to Eq. (1).

$$A = A_0 e^{-k_{obs} t} + A_\infty \quad (1)$$

The corresponding pseudo-first order rate constants, k_{obs}, exhibit linear dependence on the concentration of HOCl (Fig. S2), i.e., the oxidation of the amino acids occurs in an overall second order process (Eq. 2).

$$dc_{MC}/dt = k_f\, c_{HOCl}\, c_{AA} \quad (2)$$

(MC: mono-*N*-chloro amino acid; AA: amino acid).

The corresponding second order rate constants of the formation of mono-*N*-chloro compounds (k_f) at $c^-_{OH} = 0.05$ M, $k_f = 575 \pm 11$ and 453 $\pm$ 6 $M^{-1}s^{-1}$, are in excellent agreement with the results reported earlier for the formation of MCG and MCA at amino acid excess under the same conditions, 569 and 483 $M^{-1}s^{-1}$, respectively.[43] Thus, the initial reaction was assigned to the formation of the mono-chlorinated derivatives and the ^{1}H NMR spectra corroborates this assumption (vide infra).

At longer reaction times, the absorbance significantly decreases at the characteristic absorbance band of OCl^- (λ_{max} = 292 nm) in both systems (Fig. 1).

The concentration of the remaining HOCl was calculated from the absorbance at the end of the reaction and plotted as a function of the initial HOCl concentration in Fig. 2. These plots confirm that 1 mol Gly and 1 mol Ala consume 3.4 and 3.3 moles HOCl, respectively.

In the case of Ala, the absorbance decay was recorded at two different wavelengths (260 and 290 nm) and could be fitted to a simple first order expression (Eq. 1, Fig. S3). The first-order rate constant of the decomposition (k_d^{ala}) is practically independent of the HOCl concentration, $k_d^{ala} = (8.1 \pm 0.9) \times 10^{-4}\ s^{-1}$ (Fig. S4).

Upon mixing Ala and HOCl at high pH, the first recorded ^{1}H NMR spectrum at 3 min features a doublet and a quartet at 1.25 and 3.51 ppm, respectively (Fig. 3). In accordance with our previous studies, these peaks are assigned to *N*-chloro-α-alanine and marked as MCA_1 and MCA_2 in the spectra.[40] As a consequence of using the water suppression method in the NMR experiments, the intensities of peaks are significantly reduced in the vicinity of the water peak (~4.8 ppm) i.e., in the 3.0 – 6.6 ppm region. Thus, the MCA_2 peak is considerably smaller than expected but proportional to the concentration of MCA.

Peaks related to *N, N*-dichloro alanine (DCA) are absent from the spectrum confirming that this species does not form under such conditions. Time resolved NMR spectra confirm the relatively slow decay of MCA, the formation of acetonitrile (AcCN: 2.05 ppm, singlet) and *N*-chloro acetamide (Cl-Acam: 1.88 ppm, singlet) as main products, and acetate ion (Ac: 1.90 ppm, singlet), acetaldehyde (Aca, diol: 1.31 ppm, doublet, Aca, aldehyde: 2.22 ppm, doublet), chloroacetaldehyde (Cl-Aca: 8.43 ppm, singlet), chloroform ($CHCl_3$: 7.66 ppm, singlet) at

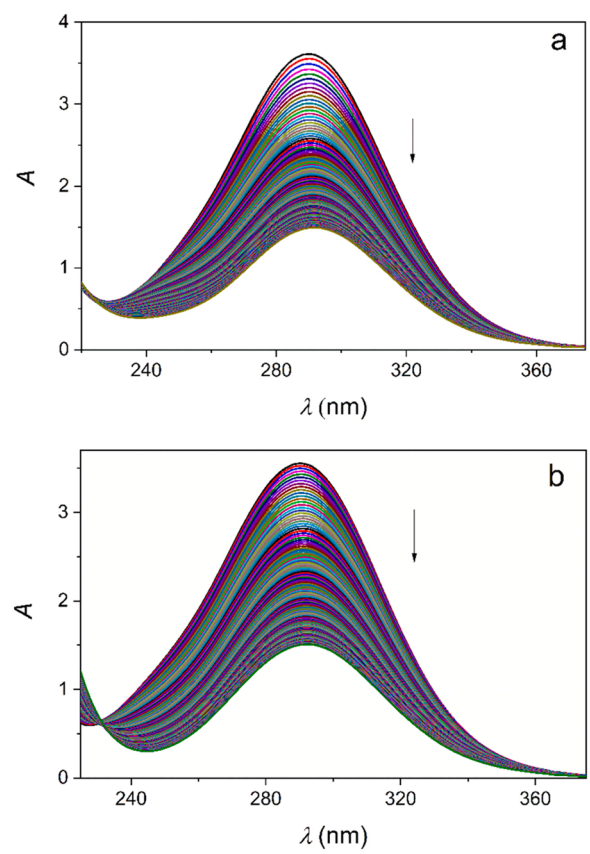

Fig. 1. Time resolved spectral changes recorded during the chlorination of Gly (a) and Ala (b) by excess HOCl under alkaline conditions. $c^0_{aa} = 2.50 \times 10^{-3}$ M, $c^0_{HOCl} = 1.25 \times 10^{-2}$, $c^-_{OH} = 5.00 \times 10^{-2}$ M, $I = 1.0$ M ($NaClO_4$), $T = 25.0$ °C, a: $t = 3600$ s, $\Delta t = 15$ s, b: $t = 6000$ s, $\Delta t = 28$ s. The spectra are normalized to 1.00 cm.

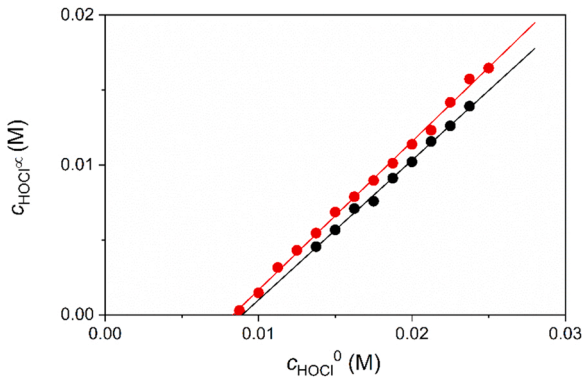

Fig. 2. The residual concentration of HOCl at the end of the reaction as a function of the initial HOCl concentration under alkaline conditions in the case of MCG (black) and MCA (red). Slope: 0.99 ± 0.01 (MCG), 0.93 ± 0.02 (MCA) $c^0_{aa} = 2.50 \times 10^{-3}$ M, $c^-_{OH} = 5.00 \times 10^{-2}$ M, $I = 1.0$ M ($NaClO_4$), $T = 25.0$ °C.

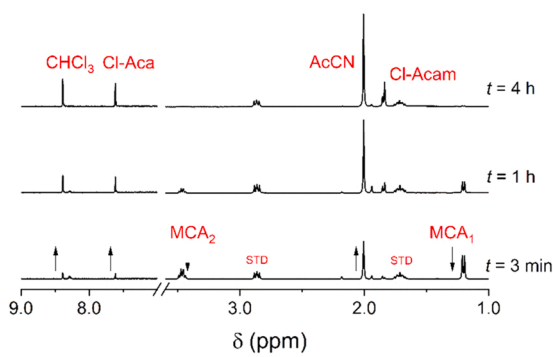

Fig. 3. Time-dependent ^{1}H NMR spectra during the decomposition reaction of MCA under alkaline conditions. The arrows indicate the changes of intensities. $c^0_{ala} = 7.50 \times 10^{-3}$ M, $c^0_{HOCl} = 3.75 \times 10^{-2}$, $c^-_{OH} = 5.00 \times 10^{-2}$ M, $T = 25.0$ °C.

relatively low concentration levels. The formation and subsequent decay of acetamide (Acam: 1.98 ppm, singlet) and *N*-chloro ethanimine (Cl-Etim: 8.33 ppm, quartet) were also confirmed. Whenever it was feasible, the ^{1}H NMR spectrum of a species was recorded individually to confirm the assignment of the peaks (e.g., Fig. S5).

As shown in Fig. 4, the intensities of the characteristic peaks of MCA (MCA_1, MCA_2), AcCN and Cl-Acam as a function of time can be fitted to a single exponential function (Eq. 1).

Although the ionic strength was not set in the ^{1}H NMR experiments, the values of k_d determined from the spectrophotometric and the NMR measurements for the decay of MCA are in excellent agreement: $k_{d,MCA1} = (7.5 \pm 0.4) \times 10^{-4}$ s^{-1} $k_{d,MCA2} = (8.4 \pm 0.4) \times 10^{-4}$ s^{-1} and $k^{ala}_{d290\ nm} = (7.85 \pm 0.01) \times 10^{-4}$ s^{-1}. According to our recent study, the decomposition of MCA proceeds via a pH independent and an OH^- assisted path, $k_d = k + k_{OH}[OH^-]$. The values of k^{ala}_d obtained here and reported earlier at 0.05 M $[OH^-]$ agree reasonably well.[40].

The fit of the AcCN and Cl-Acam peaks as a function of time yields $k_{f,AcCN} = (8.1 \pm 0.8) \times 10^{-4}$ s^{-1} and $k_{f,Cl\text{-}Acam} = (3.3 \pm 0.5) \times 10^{-4}$ s^{-1} for the formation of these species. The results are consistent with the rate determining decomposition of MCA and subsequent fast transformation of the intermediates via oxidation by the excess HOCl. The about 2.5 times difference in the rate constants for the formation of the two main products suggests that they form via different reaction paths. In the case of the minor products, the fit of the NMR kinetic traces yields rate constants in the range of (5.6 – 6.2) × 10^{-4} s^{-1} with ± 20% uncertainty. Because of the small intensities, these kinetic results should be considered semi-quantitative. However, the results undoubtedly confirm that their formation is relatively fast from the intermediate formed in the rate determining step.

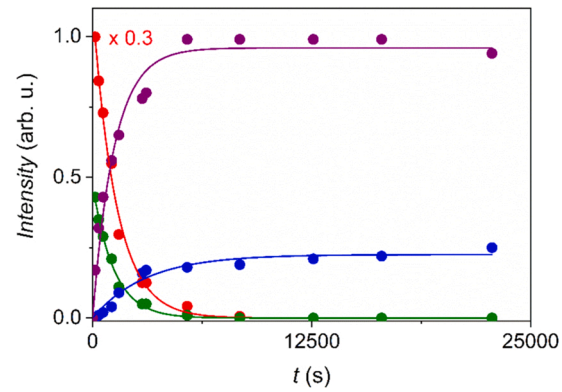

Fig. 4. The intensities of the characteristic ^{1}H NMR peaks of MCA (● 3.51 ppm, ● 1.25 ppm), AcCN (● 2.05 ppm) and Cl-Acam (● 1.88 ppm) as a function of time. Solid lines: fitted traces to a first-order rate expression. $c^0_{ala} = 7.50 \times 10^{-3}$ M, $c^0_{HOCl} = 3.75 \times 10^{-2}$, $c^-_{OH} = 5.00 \times 10^{-2}$ M, $T = 25.0$ °C.

It is reasonable to assume that the overall reaction proceeds as outlined in Scheme 1. As proposed earlier, MCA is involved in a fast acid – base pre-equilibrium yielding a carbanion at high pH, the corresponding equilibrium constant is K_{OH} [40]. Via the pH independent path, the rate determining dechlorination of MCA (k) is followed by decarboxylation and the formation of ethanimine. In subsequent fast hydration, hydrolytic and chlorination steps, this compound is converted into Acam which is chlorinated to form the *N*-chloro derivative, Cl-Acam, in the final step.

The dechlorination of the carbanionic form of MCA leads to the formation of imino-propionate in a rate determining step (k_1 i.e., $k_{OH} = k_1 K_{OH}$). *N*-chlorination of this imine is followed by decarboxylation and the formation the carbanionic form of *N*-chloro ethanimine. While spontaneous decomposition of this ion yields AcCN, its protonation and subsequent hydration leads to the formation of Aca. Further oxidation reactions with OCl^- transform Aca into the final products.

The oxidation of glycine shows similar patterns however the transformation of MCG cannot be descried with a simple first-order process (Fig. 5). The kinetic traces were fitted to a double exponential function (Eq. 3).

$$A = A_1 e^{-k_{obs1} t} + A_2 e^{-k_{obs2} t} + A_\infty \quad (3)$$

In control experiments, MCG was prepared by mixing glycine with equivalent amount of HOCl in slightly alkaline solution. Under such conditions MCG forms immediately and stable for an extended period. When this solution was reacted with excess HOCl, the same kinetic features were observed. The corresponding first order rate constants do not depend on the concentration of HOCl (Fig. S6) confirming again that HOCl is not involved in the rate determining step of the further transformation of MCG.

In the alkaline reaction mixture of glycine and excess HOCl, the singlet at 3.57 ppm corresponds to the CH_2 protons of MCG (Fig. 6).[42] This peak disappears, and a new singlet develops at 8.43 ppm which corresponds to the formation of formamide (FA). The assignment of the new peak was confirmed in an independent experiment by recording the spectrum of a formamide solution.

As shown in Fig. 7, the degradation of MCG and the formation of FA follow first order kinetics. The calculated decomposition(k_d) and formation (k_f) rate constants are in excellent agreement with each other, and the bigger rate constants obtained from the spectrophotometric measurements at 290 nm: $k_{d,MCG} = (2.41 \pm 0.05) \times 10^{-3}$ s^{-1}, $k_{f,FA} = (2.95 \pm 0.19) \times 10^{-3}$ s^{-1}, $k_{d1}{}^{gly}{}_{,290\ nm} = (2.63 \pm 0.01) \times 10^{-3}$ s^{-1}. Noticeably, MCG decomposes faster than MCA. As discussed earlier, this difference is due to the positive inductive effect of the methyl substituent in alanine that increases the basicity of the α-carbon atom [40]. Consequently, the formation of the carbanion is less favorable and the rate determining step

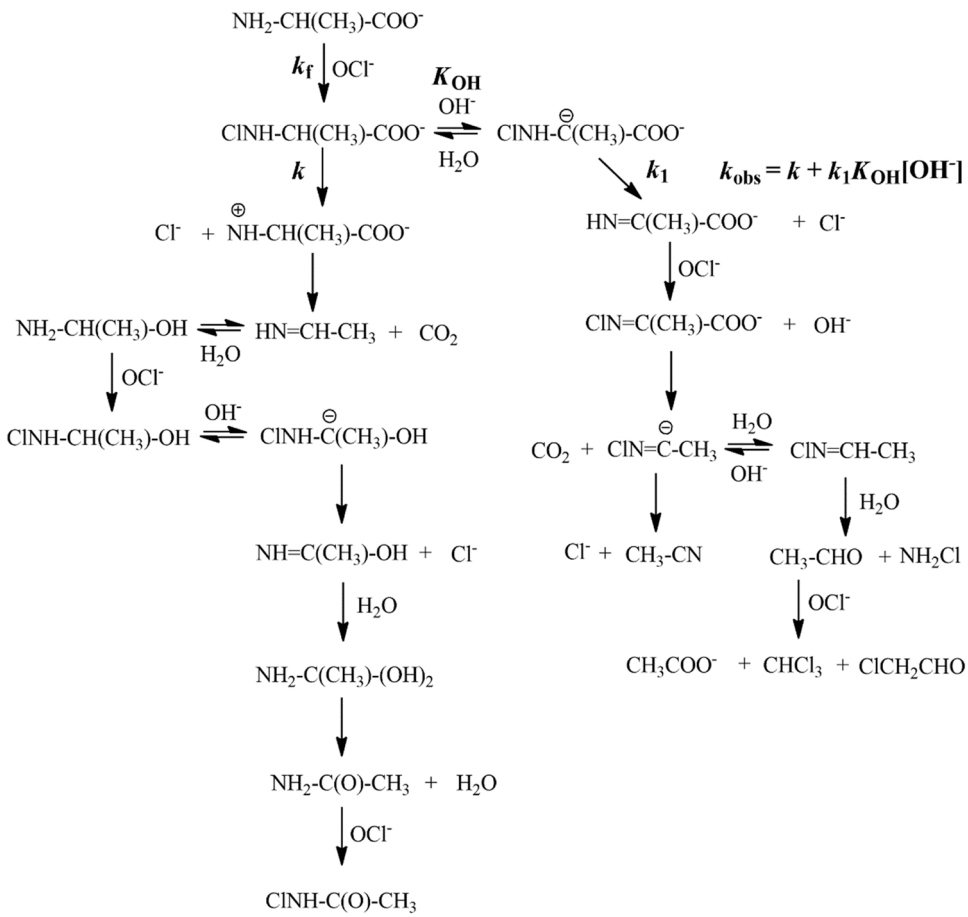

Scheme 1. The mechanism of the chlorination of α-alanine under alkaline conditions.

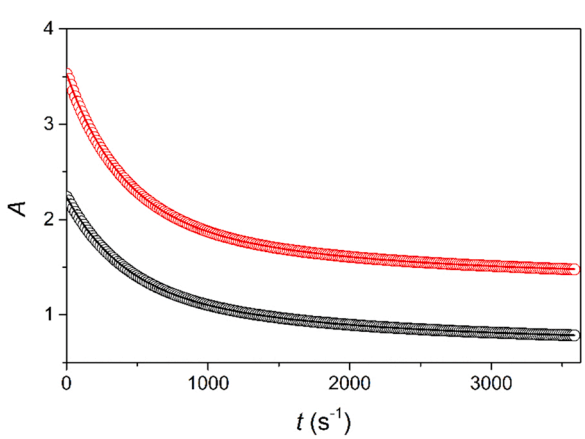

Fig. 5. Typical experimental (markers) and fitted (continuous lines) kinetic traces for the chlorination of MCG at different wavelengths under alkaline conditions. The traces were fitted to Eq. (3). The kinetic traces are normalized to 1.00 cm optical pathlength. $c^0_{gly} = 2.50 \times 10^{-3}$ M, $c^0_{HOCl} = 1.25 \times 10^{-2}$, $c^-_{OH} = 5.00 \times 10^{-2}$ M, $I = 1.0$ M ($NaClO_4$), $T = 25.0$ °C, $t = 3600$ s, $\Delta t = 15$ s, $\lambda = 290$ (●), and 260 (•) nm.

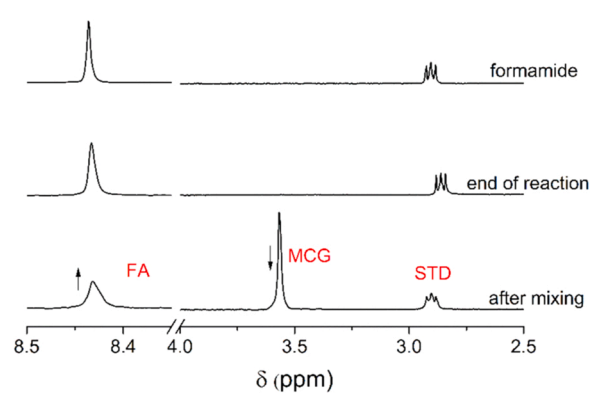

Fig. 6. Time - dependent ^{1}H NMR spectra during the chlorination of MCG and the formamide spectra under alkaline conditions. $c^0_{gly} = 7.50 \times 10^{-3}$ M, $c^0_{HOCl} = 3.75 \times 10^{-2}$, $c^0_{FA} = 2.50 \times 10^{-3}$ M, $c^-_{OH} = 5.00 \times 10^{-2}$ M, $T = 25.0$ °C.

becomes slower in the case of Ala. According to ion chromatographic experiments, about 50% of MCG is converted to OCN^-, which forms in a first-order process (Fig.S7). The corresponding rate constant, $k^-_{f,OCN} = (1.24 \pm 0.15) \times 10^{-3}\,s^{-1}$, is about 30% higher than the smaller rate constant from spectrophotometry, $k^{gly}_{290\,nm} = (6.39 \pm 0.09) \times 10^{-4}\,s^{-1}$. This is a reasonable agreement by considering that the ionic strength was not set in the ion chromatographic experiments in order to avoid complications with ion suppressed conductometric detection.

This strongly suggests again that the overall process is controlled by the initial decomposition of MCG that occurs only via the OH^--assisted path [42]. The transformation of carbanionic form of MCG is very similar to that of MCA (Scheme 2). Thus, dechlorination of the carbanion leads to the formation of iminoacetate in a rate determining step. Subsequent fast reactions yield the *N*-chloro methanimine carbanion which decomposes into CN^-. In the excess of OCl^-, cyanide ion is oxidized to OCN^- via the formation of CNCl. The competing protonation of the carbanion followed by hydration and dechlorination steps leads to the formation of FA. This sequence differs from the corresponding part of

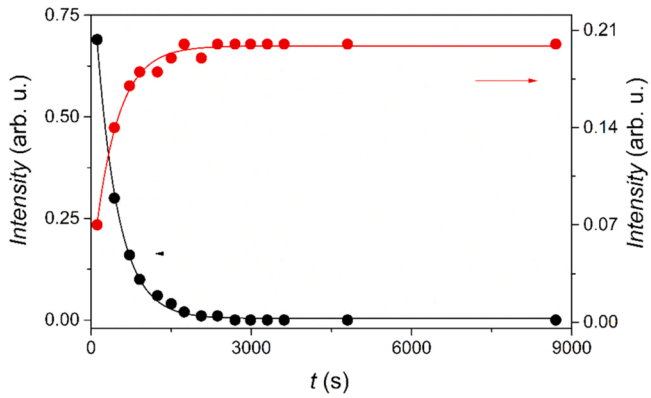

Fig. 7. The intensity of the characteristic ^{1}H NMR peaks of MCG (• 3.57 ppm) and FA (● 8.43 ppm) as a function of time. $c^0_{gly} = 7.50 \times 10^{-3}$ M, $c^0_{HOCl} = 3.75 \times 10^{-2}$, $c^0_{FA} = 2.50 \times 10^{-3}$ M, $c_{\overline{OH}} = 5.00 \times 10^{-2}$ M, $T = 25.0$ °C.

the MCA mechanism where the N–C double bond of *N*-chloro ethanimine breaks upon hydration most likely due to the inductive effect of the methyl group.

3.2. Neutral conditions

Under neutral conditions, the addition of excess HOCl to the amino acids is also associated with a complex kinetic pattern. The leftover HOCl concentrations in the spent reaction mixtures correspond to the consumption of 2.7 and 5.2 moles of HOCl by one mole Ala and Gly, respectively (Fig. S8). In both cases, an absorbance jump was observed in the kinetic traces within the dead-time of the stopped-flow instrument. In accordance with our earlier results, this is due to the formation of the mono-*N*-chloro amino acid [43].

In the case of alanine, time resolved spectra reveal two partially overlapping first order processes that complete well within a minute (Fig. S9). The corresponding rate constants were obtained by fitting the kinetic traces at 240 nm to Eq. 3. These observations can be explained by the quick oxidation of MCA to DCA (k_{obs1}) and the conversion of the dichloro derivative (k_{obs2}) into a relatively stable intermediate which is involved in a considerably slower subsequent process.

The total concentration of HOCl was corrected by the amount consumed during the initial fast formation of the mono-chloro species (one equivalent of the amino acid) to obtain c^{cor}_{HOCl}. The plot of k_{obs1}/c^{cor}_{HOCl} as a function of c^{cor}_{HOCl} is a straight line with zero intercept confirming that the faster step is second order in hypochlorous acid (Fig. 8), i.e., the formation of DCA is an overall third-order process.

The second order dependence on HOCl can be rationalized by considering that chlorine monoxide, Cl_2O, is always present at a relatively low concentration level in a HOCl solution [4,41]. Provided that these two species are always in fast pre-equilibrium and Cl_2O reacts much faster with the substrate than HOCl, the experimentally observed kinetic feature is expected. The high reactivity of Cl_2O toward organic substrates has been reported before [15,41]. The second rate constant does not depend on the HOCl concentration. Thus, the kinetic model detailed in eq.s. (4–7) provides adequate interpretation of these observations.

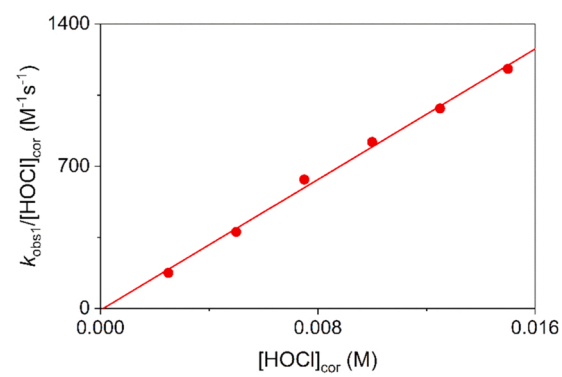

Fig. 8. The dependence of k_{obs1} on the concentration of HOCl under neutral conditions in the Ala – HOCl system. $c^0_{ala} = 5.00 \times 10^{-4}$ M, pH = 6.74, $I = 1.0$ M ($NaClO_4$), $T = 25.0$ °C.

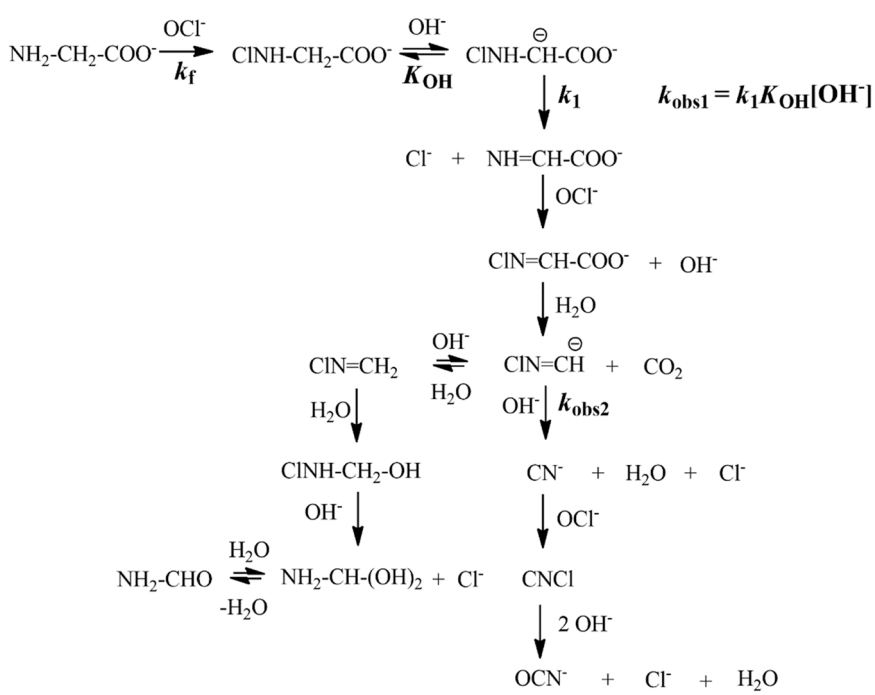

Scheme 2. The mechanism of the chlorination of glycine under alkaline conditions.

$$2HOCl \rightleftharpoons Cl_2O + H_2O \quad K_1 = \frac{[Cl_2O]}{[HOCl]^2} \tag{4}$$

$$Ala + HOCl = MCA + H_2O \text{ very fast} \tag{5}$$

$$MCA + Cl_2O = DCA + HOCl \; k_{Cl2O} \tag{6}$$

$$DCA \rightarrow Int_1 \; k_2 \tag{7}$$

thus, $k_{obs1} = k_{Cl2O}\, K_1\, [HOCl]^2$ and $k_{obs2} = k_2$. Evaluation of the kinetic traces yields $k_{Cl2O}\, K_1 = (8.0 \pm 0.3) \times 10^4\ M^{-1}s^{-1}$ and $k_2 = 0.29 \pm 0.01\ s^{-1}$.

According to the time resolved ^{1}H NMR spectra (Fig. 9), the final products of his reaction are acetonitrile (AcCN: 2.05 ppm, singlet) and acetate ion (Ac: 1.90 ppm, singlet). Acetaldehyde (Aca, diol: 1.31 ppm, doublet; Aca, aldehyde: 2.22 ppm, doublet and 9.65 ppm, quartet), *N*-chloro ethanimine (Cl-Etim: 2.05 ppm, doublet and 8.33 ppm, quartet) and its hydrated form, *N*-chloro-1-aminoethanol (Cl-Amet: 1.46 ppm, doublet) were detected as transient species.

The mechanism postulated in Scheme 3 is fully consistent with the experimental results. After the fast two-step chlorination of Ala, DCA undergoes decarboxylation and partial dechlorination. These processes are relatively fast and DCA cannot be detected even in the first NMR spectrum recorded about 3 min after mixing the reactants. The immediate product of the decomposition is Cl-Etim. The decay of this species can easily be monitored by ^{1}H NMR spectroscopy, its half-life is about 30 min (Fig. S10). Cl-etim either decomposes spontaneously into AcCN, or undergoes hydration and produces Aca via the formation of Cl-Amet. Finally, the aldehyde is oxidized to acetate ion. Because of the competing reaction paths the decomposition of Cl-etim is about two times faster than the formation of Ac.

Under neutral conditions, the chlorination of Gly exhibit distinct features compared to that of Ala. After the formation of MCG within the dead-time of the stopped-flow instrument, three partly overlapping kinetic processes were observed in the first 10 min of the overall reaction (Fig. S11). The kinetic traces could be fitted to a treble exponential function at 5–25 times excess of HOCl. However, the kinetic traces are not very well defined for fitting the parameters of the two slower steps and the results are inconlcusive as far as the HOCl concentration dependencies of k_{obs2} and k_{obs3} are concerned. In accordance with the Ala system, we assign the first step to the conversion of MCG to DCG. The HOCl concentration dependence of k_{obs1} reveals that the chlorination occurs with Cl_2O, i.e., $k_{obs1} = k_{Cl2O}\, K_1\, [HOCl]^2$ and $k_{Cl2O}\, K_1 = (8.7 \pm 0.3) \times 10^4\ M^{-1}s^{-1}$ (Fig. 10). It is remarkable that the rate constants for the reactions of MCG and MCA with Cl_2O are practically the same, i.e., the alkyl substituent in α-position does not affect the chlorination process.

The peaks in the ^{1}H NMR spectrum recorded just after mixing the reactants were assigned to *N*-chloro methanimine (Cl-Metim: 7.95 ppm, double doublet) and *N*-chloro aminomethanol (Cl-Ammet: 4.30 ppm, singlet) (Fig. 11). These peaks disappear as the reaction proceeds indicating the transformation of each organic compound into inorganic species. Ion chromatographic experiments confirm the transient formation of OCN^- in this system (Fig. S12).

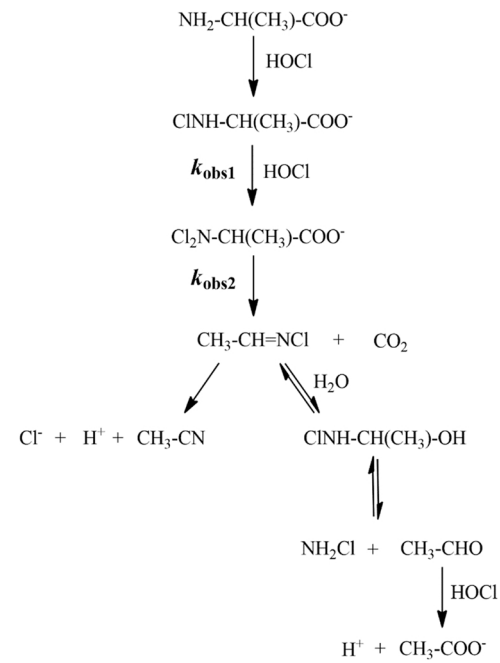

Scheme 3. The mechanism of the chlorination of α-alanine under neutral conditions.

The proposed mechanism for the overall process is shown in Scheme 4. The initial part of the chlorination of Gly is the same as that of Ala. The decomposition of Cl-Metim proceeds via two competing reaction paths. Its spontaneous decomposition yields CN^- which is immediately converted to OCN^-. The latter is oxidized by HOCl to HCO_3^-, Cl^- and N_2 in a relatively slow reaction. In analogy with the Ala system, the appearance of Cl-Ammet implies that NH_2Cl and CH_2O also form from Cl-Metim via two equilibrium steps. The mechanisms predicts that these species eventually disappear from the system as the corresponding equilibria shift backward and Cl-Metim is fully consumed via the irreversible other path. While we could not find direct experimental evidence for the transient formation of NH_2Cl and CH_2O, additional experiments corroborate the postulated mechanism. Monochloramine was prepared and reacted with formaldehyde in 1: 1 ratio. As shown in Fig. 11, the ^{1}H NMR spectrum of this reaction mixture features the peaks

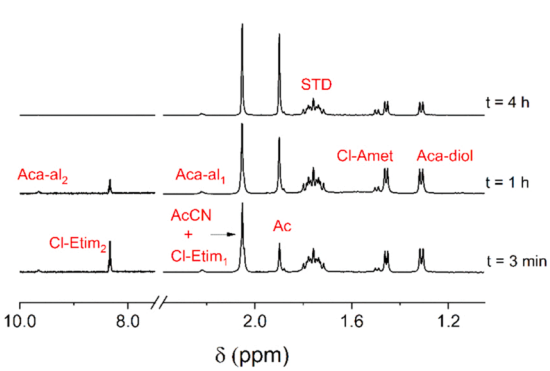

Fig. 9. Time - dependent ^{1}H NMR spectra during the decomposition reaction of DCA under neutral conditions. $c^0_{ala} = 7.50 \times 10^{-3}$ M, $c^0_{HOCl} = 3.75 \times 10^{-2}$, pH = 7.01, $T = 25.0$ °C.

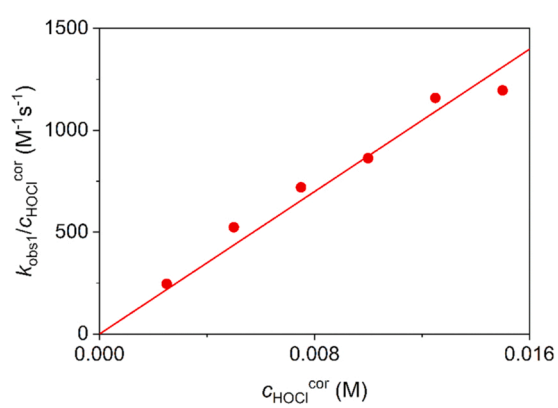

Fig. 10. The dependence of k_{obs1} on the concentration of HOCl under neutral conditions in the Gly – HOCl system. $c^0_{gly} = 5.00 \times 10^{-4}$ M, pH = 6.91, $I = 1.0$ M ($NaClO_4$), $T = 25.0$ °C.

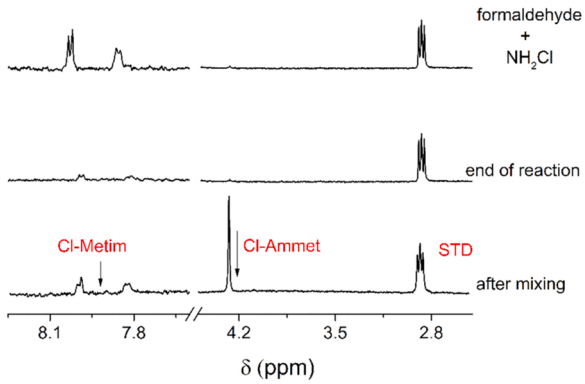

Fig. 11. ^{1}H NMR spectra during the decomposition reaction of DCG and the formaldehyde – monochloramine reaction under neutral conditions. $c^0_{gly} = 7.50 \times 10^{-3}$ M, $c^0_{form} = 2.50 \times 10^{-3}$ M, $c^0_{NH2Cl} = 2.50 \times 10^{-3}$ M, pH = 7.01, $T = 25.0$ °C.

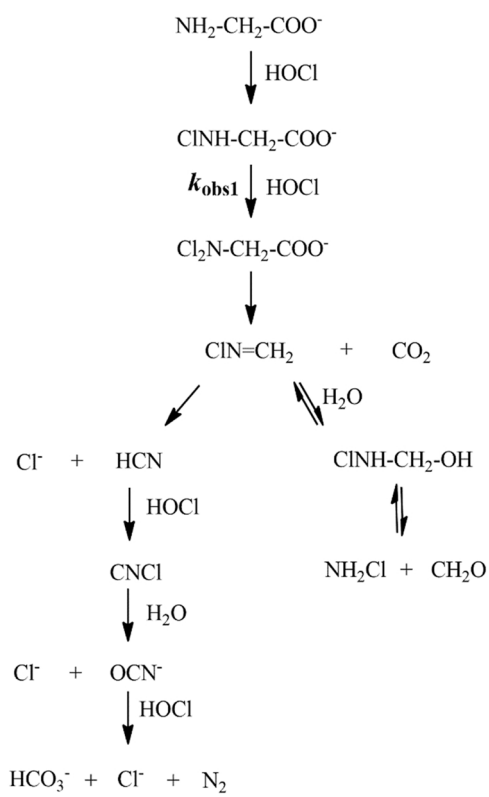

Scheme 4. The mechanism of the chlorination of glycine under neutral conditions.

of Cl-Metim and its hydrated form proving the feasibility of the equilibria among the corresponding species. Upon addition HOCl to this reaction mixture in excess, the transient formation of OCN^- was also confirmed (Fig. S13).

4. Conclusions

The chlorination of the two simplest amino acids proceeds via complex mechanisms, exploring their intimate details requires the use of combined kinetic and spectroscopic experimental methods. These reactions show distinct characteristics under neutral and alkaline conditions. At high pH, the common feature of the two systems is that the *N*-dichloroamino carboxylate ion does not form and the overall process is controlled by the initial decomposition of the *N*-monochloro derivative. The formation of carbanions opens alternative reaction paths, and the overall process shows more complexity compared to neutral conditions. Subsequent reaction steps include hypochlorite ion as a mild oxidant and produce oxo compounds and chlorinated species. Under neutral conditions, monochloroamino acid form immediately and converted into the dichloroamino acid by Cl_2O in a fast process. In further reaction steps, high oxidation state products form and the reaction proceeds to full mineralization in the case of glycine.

The results confirm that there is a mechanistic changeover when the pH is changed from neutral to alkaline. The limiting mechanisms established at pH 7 and 12.3 contribute to the overall process in a well-defined pH dependent manner making possible to predict the kinetic features in this pH range. Due to the combination of the limiting mechanisms, the reactions become exceedingly complex and meticulous mechanistic studies are not feasible under slightly alkaline conditions. However, pH dependent ^{1}H NMR spectra recorded at 3 min after mixing the reactants in the α-alanine system serve clear evidence that the two mechanisms are simultaneously operative in the intermediate pH range (Fig. S14).

Due to the α-CH_3 group in alanine, the two systems differ significantly as far as the intermediates and final products are concerned. This suggests that the chlorination of other amino acids needs to be investigated on a case-by-case basis. Nevertheless, some of the results presented here are also relevant in the other systems. Thus, the interplay of two mechanisms with the same reactive forms of the oxidants identified here, Cl_2O and HOCl, are expected to govern the overall chlorination processes of amino acids and various amines in the neutral – alkaline pH range.

The compounds formed from alanine ($CHCl_3$, chloro acetaldehyde, N-chloroacetamide) and glycine (formamide, thiocyanate) at high pH are considered to be toxic. Less toxic compounds form under neutral conditions. However, some of the intermediates have extended lifetime in these systems and they may also react with other components of raw water during water treatment processes. The potential risks associated with such reactions should be clarified in detail.

Environmental implication

In source waters, amino acids account for about 75% of the total dissolved nitrogen. Therefore, it is an essential issue how the reactions of these compounds with hypochlorite ion can be controlled to avoid the formation of toxic compounds. The compounds formed from alanine ($CHCl_3$, chloro acetaldehyde, N-chloroacetamide) and glycine (formamide, cyanate) at high pH are considered to be toxic. Less toxic compounds form under neutral conditions. However, some of the intermediates have extended lifetime in these systems and they may also react with other components of raw water during water treatment processes.

CRediT authorship contribution statement

Fruzsina Simon: Investigation, Formal analysis, Visualization, Writing – review & editing, **Mária Szabó:** Conceptualization, Investigation, Formal analysis, Writing – original draft, Writing – review & editing, **István Fábián:** Conceptualization, Writing – original draft, Writing – review & editing, Supervision, Funding acquisition.

Declaration of Competing Interest

The authors declare the following financial interests/personal relationships which may be considered as potential competing interests: István Fábián reports financial support was provided by National, Research, Development and Innovation Office.

Data availability

Data will be made available on request.

Acknowledgement

This study was supported by the National Research, Development and Innovation Found of Hungary under grant number OTKA-139140.

Appendix A. Supporting information

Supplementary data associated with this article can be found in the online version at doi:10.1016/j.jhazmat.2023.130794.

References

[1] Ackerson, N.O.B., Killinger, A.H., Liberatore, H.K., Ternes, T.A., Plewa, M.J., Richardson, S.D., Duirk, S.E., 2019. Impact of chlorine exposure time on disinfection byproduct formation in the presence of iopamidol and natural organic matter during chloramination. J Environ Sci 78, 204–214.
[2] Adam, L.C., Fábián, I., Suzuki, K., Gordon, G., 1992. Hypochlorous acid decomposition the pH 5-8 region. Inorg Chem 31 (17), 3534–3541.
[3] Adams, R.W., Holroyd, C.M., Aguilar, J.A., Nilsson, M., Morris, G.A., 2013. "Perfecting" WATERGATE: clean proton NMR spectra from aqueous solution. Chem Commun 49 (4), 358–360.
[4] Beach, M.W., Margerum, D.W., 1990. Kinetics of oxidation of tetracyanonickelate (II) by chlorine monoxide, chlorine, and hypochlorous acid and kinetics of chlorine monoxide formation. Inorg Chem 29 (6), 1225–1232.
[5] Bond, T., Huang, J., Templeton, M.R., Graham, N., 2011. Occurrence and control of nitrogenous disinfection by-products in drinking water - A review. Water Res 45 (15), 4341–4354.
[6] Cai, L., Yu, S., Li, L., 2022. Formation of odorous aldehydes, nitriles and N-chloroaldimines from free and combined leucine during chloramination. Water Res 210, 117990.
[7] Cai, L.Y., Li, L., Yu, S.L., 2020. Formation of odorous aldehydes, nitriles and N-chloroaldimines from combined leucine in short oligopeptides during chlorination. Water Res 177, 115803.
[8] Caravati, E.M., Litovitz, T.L., 1988. Pediatric cyanide intoxication and death from acetonitrile-containing cosmetic. Jama-J Am Med Assoc 260 (23), 3470–3473.
[9] Deborde, M., von Gunten, U., 2008. Reactions of chlorine with inorganic and organic compounds during water treatment - Kinetics and mechanisms: A critical review. Water Res 42 (1–2), 13–51.
[10] Dotson, A., Westerhoff, P., Krasner, S.W., 2009. Nitrogen enriched dissolved organic matter (DOM) isolates and their affinity to form emerging disinfection by-products. Water Sci Technol 60 (1), 135–143.
[11] Edwards, J.O., Erstfeld, T.E., Ibnerasa, K.M., Levey, G., Moyer, M., 1986. Reaction-rates for nucleophiles with cyanogen chloride - comparison with 2 other diagonal carbon-compounds. Int J Chem Kinet 18 (2), 165–180.
[12] Englert, R.P., Shacter, E., 2002. Distinct modes of cell death induced by different reactive oxygen species - Amino acyl chloramines mediate hypochlorous acid-induced apoptosis. J Biol Chem 277 (23), 20518–20526.
[13] Fábián, I., Gordon, G., 1991. Complex-formation reactions of the chlorite ion. Inorg Chem 30 (19), 3785–3787.
[14] Fábián, I., Lente, G., 2010. Light-induced multistep redox reactions: The diode-array spectrophotometer as a photoreactor. Pure Appl Chem 82 (10), 1957–1973.
[15] Gan, W.H., Ge, Y.X., Zhong, Y., Yang, X., 2020. The reactions of chlorine dioxide with inorganic and organic compounds in water treatment: kinetics and mechanisms. Environ Sci Water Res Technol 6 (9), 2287–2312.
[16] Geller, R.J., Ekins, B.R., Iknoian, R.C., 1991. Cyanide toxicity from acetonitrile containing false nail remover. Am J Emerg Med 9 (3), 268–270.
[17] Hawkins, C.L., Pattison, D.I., Davies, M.J., 2002. Reaction of protein chloramines with DNA and nucleosides: evidence for the formation of radicals, protein-DNA cross-links and DNA fragmentation. Biochem J 365, 605–615.
[18] How, Z.T., Busetti, F., Linge, K.L., Kristiana, I., Joll, C.A., Charrois, J.W.A., 2014. Analysis of free amino acids in natural waters by liquid chromatography–tandem mass spectrometry. J Chromatogr A 1370, 135–146.
[19] How, Z.T., Kristiana, I., Busetti, F., Linge, K.L., Joll, C.A., 2017. Organic chloramines in chlorine-based disinfected water systems: a critical review. J Environ Sci 58, 2–18.
[20] How, Z.T., Linge, K.L., Busetti, F., Joll, C.A., 2016. Organic chloramines in drinking water: an assessment of formation, stability, reactivity and risk. Water Res 93, 65–73.
[21] How, Z.T., Linge, K.L., Busetti, F., Joll, C.A., 2017. Chlorination of amino acids: reaction pathways and reaction rates. Environ Sci Technol 51 (9), 4870–4876.
[22] How, Z.T., Linge, K.L., Busetti, F., Joll, C.A., 2018. Formation of odorous and hazardous by-products from the chlorination of amino acids. Water Res 146, 10–18.
[23] Hrudey, S.E., 2009. Chlorination disinfection by-products, public health risk tradeoffs and me. Water Res 43 (8), 2057–2092.
[24] Hu, J.L., Chu, W.H., Sui, M.H., Xu, B., Gao, N.Y., Ding, S.K., 2018. Comparison of drinking water treatment processes combinations for the minimization of subsequent disinfection by-products formation during chlorination and chloramination. Chem Eng J 335, 352–361.
[25] Irving, H., Miles, M., Pettit, L., 1967. A study of some problems in determining the stoicheiometric proton dissociation constants of complexes by potentiometric titrations using a glass electrode. Anal Chim Acta 38, 475–488.
[26] Kim, J., Chung, Y., Shin, D., Kim, M., Lee, Y., Lim, Y., Lee, D., 2003. Chlorination by-products in surface water treatment process. Desalination 151 (1), 1–9.
[27] Kulcharyk, P.A., Heinecke, J.W., 2001. Hypochlorous acid produced by the myeloperoxidase system of human phagocytes induces covalent cross-links between DNA and protein. Biochemistry 40 (12), 3648–3656.
[28] Laingam, S., Froscio, S.M., Bull, R.J., Humpage, A.R., 2012. In vitro toxicity and genotoxicity assessment of disinfection by-products, organic N-chloramines. Environ Mol Mutagen 53 (2), 83–93.
[29] Liu, M., Mao, X.-a, Ye, C., Huang, H., Nicholson, J.K., Lindon, J.C., 1998. Improved WATERGATE Pulse Sequences for Solvent Suppression in NMR Spectroscopy. J Magn Reson 132 (1), 125–129.
[30] Mateus, F.H., Lepera, J.S., Lanchote, V.L., 2005. Determination of acetonitrile and cyanide in rat blood: application to an experimental study. J Anal Toxicol 29 (2), 105–109.
[31] Microcal 2018 OriginPro 2018b, Microcal Software Inc., Northampton, MA.
[32] Na, C.Z., Olson, T.M., 2004. Stability of cyanogen chloride in the presence of free chlorine and monochloramine. Environ Sci Technol 38 (22), 6037–6043.
[33] Na, C.Z., Olson, T.M., 2006. Mechanism and kinetics of cyanogen chloride formation from the chlorination of glycine. Environ Sci Technol 40 (5), 1469–1477.
[34] Pedersen, E.J., Marinas, B.J., 2001. The hydroxide-assisted hydrolysis of cyanogen chloride in aqueous solution. Water Res 35 (3), 643–648.
[35] Peintler, G., Nagypál, I., Epstein, I.R., 1990. Systematic design chemical oscillators – kinetics and mechanism of the reaction between chlorite ion and hypochlorous acid. J Phys Chem 94 (7), 2954–2958.
[36] Pero, R.W., Sheng, Y.Z., Olsson, A., Bryngelsson, C., LundPero, M., 1996. Hypochlorous acid N-chloramines are naturally produced DNA repair inhibitors. Carcinogenesis 17 (1), 13–18.
[37] Postigo, C., Andersson, A., Harir, M., Bastviken, D., Gonsior, M., Schmitt-Kopplin, P., Gago-Ferrero, P., Ahrens, L., Ahrens, L., Wiberg, K., 2021. Unraveling the chemodiversity of halogenated disinfection by-products formed during drinking water treatment using target and non-target screening tools. J Hazard Mater 401, 123681.
[38] Richardson, S.D., Plewa, M.J., Wagner, E.D., Schoeny, R., DeMarini, D.M., 2007. Occurrence, genotoxicity, and carcinogenicity of regulated and emerging disinfection by-products in drinking water: a review and roadmap for research. Mutat Res Rev Mutat Res 636 (1–3), 178–242.
[39] Shen, R., Andrews, S.A., 2011. Demonstration of 20 pharmaceuticals and personal care products (PPCPs) as nitrosamine precursors during chloramine disinfection. Water Res 45 (2), 944–952.
[40] Simon, F., Szabó, M., Fábián, I., 2019. pH controlled byproduct formation in aqueous decomposition of N-chloro-alpha-alanine. J Hazard Mater 362, 286–293.
[41] Sivey, J.D., McCullough, C.E., Roberts, A.L., 2010. Chlorine monoxide (Cl2O) and molecular chlorine (Cl-2) as active chlorinating agents in reaction of dimethenamid with aqueous free chlorine. Environ Sci Technol 44 (9), 3357–3362.
[42] Szabó, M., Baranyai, Z., Somsák, L., Fábián, I., 2015. Decomposition of N-chloroglycine in alkaline aqueous solution: kinetics and mechanism. Chem Res Toxicol 28 (6), 1282–1291.
[43] Szabó, M., Simon, F., Fábián, I., 2019. The formation of N-chloramines with proteinogenic amino acids. Water Res 165, 114994.
[44] Thurman, E.M., 1985. Organic Geochemistry of Natural Waters. Martinus Nijhoff, Dordrecht.
[45] Tonomura, B., Nakatani, H., Ohnishi, M., Yamaguchiito, J., Hiromi, K., 1978. Test reactions for a stopped-flow apparatus – reduction of 2,6-dichlorophenolindophenol and potassium ferricyanide by L-ascorbic acid. Anal Biochem 84 (2), 370–383.
[46] Westerhoff, P., Mash, H., 2002. Dissolved organic nitrogen in drinking water supplies: a review. J Water Supply Res Technol-Aqua 51 (8), 415–448.
[47] White, G.C., 1992. Handbook of Chlorination and Alternative Disinfectants. Van Nostrand Reinhold, New York.
[48] Yang, Y.L., Yu, Q., Zhou, R.N., Feng, J., Zhang, K.J., Li, X.Y., Ma, X.Y., Dietrich, A. M., 2020. Occurrence of free amino acids in the source waters of Zhejiang Province, China, and their removal and transformation in drinking water systems. Water 12 (1), 12010073.
[49] Yu, X., Goczze, Z., Cabooter, D., Dewil, R., 2021. Efficient reduction of carbamazepine using UV-activated sulfite: assessment of critical process parameters and elucidation of radicals involved. Chem Eng J 404, 126403.
[50] Zhao, Y.L., Anichina, J., Lu, X.F., Bull, R.J., Krasner, S.W., Hrudey, S.E., Li, X.F., 2012. Occurrence and formation of chloro- and bromo-benzoquinones during drinking water disinfection. Water Res 46 (14), 4351–4360.